





## Interpretation of $^{108}\text{I}$ as an odd-odd $\gamma$ -deformed proton emitter

Pooja Siwach  and P. Arumugam \*

*Department of Physics, Indian Institute of Technology Roorkee, Roorkee 247667, Uttarakhand, India*

S. Modi 

*Department of Physics, BIT Sindri, Dhanbad, Jharkhand 828121, India*

L. S. Ferreira  and E. Maglione 

*Centro de Física e Engenharia de Materiais Avançados CeFEMA, Instituto Superior Técnico, Universidade de Lisboa, Avenida Rovisco Pais, P1049-001 Lisbon, Portugal*



(Received 2 December 2020; accepted 3 March 2021; published 18 March 2021)

We have interpreted the recent observation [K. Auranen *et al.*, *Phys. Lett. B* **792**, 187 (2019)] of proton emission from  $^{108}\text{I}$ . We find that  $\gamma$  deformation is crucial to reproduce the experimental data, and have identified the decaying state as the  $1^+$  state. The effect of the residual  $np$  interaction is also discussed. With the present calculation, we establish the first microscopic description of a triaxial odd-odd proton emitter.

DOI: [10.1103/PhysRevC.103.L031303](https://doi.org/10.1103/PhysRevC.103.L031303)

**Introduction.** In a recent experiment [1] performed at Argonne National Laboratory, a weak 0.50(21)% proton decay branch from  $^{108}\text{I}$  was observed for the first time. The  $Q_p$  value and the corresponding half-life are extracted to be 597(13) keV and 5.3(22) s, respectively. This further helped in the indirect measurement of the proton separation energy of  $^{104}\text{Sb}$ . With this measurement, the possible branching in the end cycle (Sn-Sb-Te cycle shown in Figure 1) of the astrophysical rapid proton capture ( $rp$ ) process through  $^{104}\text{Sb}$  was discarded. This study supports Ref. [2] which also argued against the presence of this branching. However, the structure of  $^{108}\text{I}$  and the angular momentum of the proton emitting state are yet to be interpreted. A robust description has to consider triaxiality as learned from the case of the neighboring  $^{109}\text{I}$  [3]. With this motive, we present for the first time the theoretical study of proton emission from  $^{108}\text{I}$  using the nonadiabatic quasiparticle approach with appropriate treatment of residual  $np$  interaction.

Several theoretical approaches [5] have been applied to study proton emission, and the most consistent and reliable one is the nonadiabatic quasiparticle approach [6] based on the rotation-particle coupling. This approach has been extensively used in studying the proton emission from axially [6] and triaxially [7] deformed odd- $A$  as well as axial odd-odd nuclei [8]. Recently, it has been modified [9] to incorporate the experimental energies of even-even cores in a more microscopic way and successfully applied to triaxially deformed odd- $A$  nuclei [3]. This approach was extended to examine the structure and decay of triaxially deformed odd-odd nuclei [10]. Here, we present its extension to study triaxial odd-odd proton emitters,

which renders it the first microscopic approach to study these nuclei.

The proton emission half-life depends on the energy and angular momentum carried away by the emitted proton, along with the properties of its wave function. The odd-odd nuclei are of special interest due to the crucial role of the odd neutron, which affects the angular momentum of the emitting proton. This requires the proper treatment of the residual interaction between the valence proton and neutron. Therefore, a nonadiabatic quasiparticle approach, similar to the one used in Ref. [3] which takes into account the odd-odd nature of nuclei and triaxiality both, is needed.

**Theoretical framework.** We couple the valence proton and neutron to the triaxially deformed even-even core within the nonadiabatic quasiparticle approach. The total Hamiltonian for this system can be written as

$$H = H_{rot} + H_{intr}^p + H_{intr}^n + V_{np}, \quad (1)$$

where  $H_{rot}$  is the Hamiltonian for the triaxial rotor [9] and  $H_{intr}^{p(n)}$  accounts for the motion of the proton (neutron) in the intrinsic frame.  $V_{np}$  is the residual neutron-proton ( $np$ ) interaction. With the inclusion of the residual pairing interaction,  $H_{intr}^{p(n)}$  becomes

$$H_{intr}^{p(n)} = H_{sp}^{p(n)} + H_{pair}^{p(n)}. \quad (2)$$

where the  $H_{pair}^{p(n)}$  describes the pairing which is dealt within the BCS approach. For  $H_{sp}^{p(n)}$ , the triaxial Woods-Saxon potential is taken as the nuclear mean field potential [9] along with the spin-orbit and Coulomb potentials. Since the detailed formalism of the approach used is presented elsewhere [10], we give a brief description relevant to the present study, mainly required to calculate the rotational energies and the proton emission decay width.

\*Corresponding author: arumugam@ph.iit.ac.in

The matrix element of the total Hamiltonian given in Eq. (1) within the nonadiabatic quasiparticle coupling treatment takes the following form:

$$\begin{aligned}
 & \langle q'_p q'_n K', IM | H | q_p q_n K, IM \rangle \\
 &= (\mathcal{E}_{q_p} + \mathcal{E}_{q_n}) \delta_{KK'} \delta_{q_p q'_p} \delta_{q_n q'_n} + \sum_{j_p j_n} \sum_{j=|j_p-j_n|}^{j_p+j_n} \sum_{\Omega'_p \Omega'_n \Omega_n} \\
 & \times \sum_{\Omega'} \mathbb{W}_{KK'}^{j_p j_n j \Omega'_p \Omega'_n \Omega_n \Omega_p} \int dr f_{u_p v_p} \phi_{j_p \Omega'_p}^*(r) \phi_{j_p \Omega_p}(r) \\
 & \times \int dr f_{u_n v_n} \phi_{j_n \Omega'_n}^*(r) \phi_{j_n \Omega_n}(r) \\
 & + \delta_{KK'} f_{u_n v_n} f_{u_p v_p} \langle \psi_{p'} \psi_{n'} | V_{np} | \psi_p \psi_n \rangle, \quad (3)
 \end{aligned}$$

where the  $H$  is sandwiched between resultant states of proton, neutron, and rotor coupled systems.  $q_i$  ( $i = p$  or  $n$ ) denote the quasiparticle states,  $\mathcal{E}_{q_i}$  are the quasiparticle energies of proton and neutron, and the factor  $f_{u_i v_i} = u_i u_{i'} + v_i v_{i'}$ .  $\phi_{j_i \Omega_i}(r)$  are the single-particle wave functions comprising the radial part and mixing coefficients.  $\mathbb{W}_{KK'}^{j_p j_n j \Omega'_p \Omega'_n \Omega_n \Omega_p}$  is the matrix element of the triaxial rotor in  $K$  representation multiplied by the coupling terms, and can be expressed as

$$\begin{aligned}
 & \mathbb{W}_{KK'}^{j_p j_n j \Omega'_p \Omega'_n \Omega_n \Omega_p} \\
 &= \sum_{R R_R K'_R} A_{j_p j_n j \Omega'_p \Omega'_n R R_R}^{IK'} A_{j_p j_n j \Omega_p \Omega_n R R_R}^{IK} \sum_i C_{K_R}^{R_i} E_{T R_i} C_{K_R}^{R_i}, \quad (4)
 \end{aligned}$$

where  $E_{T R_i}$  are the rotor energies taken from the experimental data or calculated using Method 2 of Ref. [9].  $C_{K_R}^{R_i}$  are the rotor wave functions obtained by diagonalizing  $H_{rot}$  in  $R$  representation which is obtained by basis transformation from the laboratory frame to the intrinsic frame. The quantities  $A$  are coefficients having the normalization constant and the Clebsch-Gordan coefficients.

We have incorporated the residual neutron-proton interaction in the constant potential form [10] given as

$$V_{np} = (-1)^{\Sigma_p + \Sigma_n} (V_{GM} + (-1)^I (-1)^{l_p + l_n} V_N \delta_{K,0}), \quad (5)$$

where  $V_{GM}$  and  $V_N$  account for the strength of Gallagher-Moszkowski (GM) splitting (which indicates that a triplet state is energetically favored over the singlet one) [11] and Newby shift (due to which the odd spin states are favored over even spin ones belonging to  $K = 0$  band) [12], respectively. The quantity  $\Sigma_{p(n)}$  is the projection of proton (neutron) intrinsic spin on the third axis.

The wave function of the parent nucleus (initial state) is given by

$$\begin{aligned}
 \Psi_{IM} &= \sqrt{\frac{2I+1}{16\pi^2}} \sum_{\Omega_p \Omega_n \Omega K} a_{\Omega_p \Omega_n \Omega K}^I \\
 & \times [D_{MK}^I \chi_{\Omega}^{\Omega_p \Omega_n} + (-1)^{I-j_p-j_n} D_{M-K}^I R_i \chi_{\Omega}^{\Omega_p \Omega_n}], \quad (6)
 \end{aligned}$$

where  $\chi_{\Omega}^{\Omega_p \Omega_n} = \phi_{j_p \Omega_p} \phi_{j_n \Omega_n}$  is the product of single-particle wave functions obtained from the mean field calculations and  $R_i$  is the rotational operator along the second intrinsic axis.

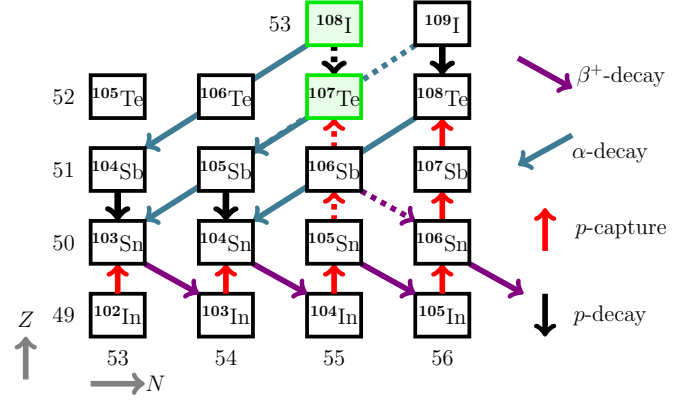


FIG. 1. Possible decay channels in the vicinity of the end cycle of the  $rp$  process as suggested in Refs. [1,2,4]. The nuclei  $^{107}\text{Te}$  and  $^{108}\text{I}$  studied in present work are highlighted in green. The weaker (stronger) decay channels are shown with dashed (solid) lines.

$a$ 's account for the amplitudes, which we obtain by solving the total Hamiltonian.

The wave function of the triaxial odd- $A$  daughter nucleus can be expressed as

$$\begin{aligned}
 \Psi_{I_d M_d} &= \sqrt{\frac{2I_d+1}{16\pi^2}} \sum_{j_n \Omega_n K_d} c_{j_n \Omega_n K_d}^{I_d} \\
 & \times [D_{M_d K_d}^{I_d} \phi_{j_n \Omega_n} + (-1)^{I_d-j_n} D_{M_d-K_d}^{I_d} \phi_{j_n, -\Omega_n}], \quad (7)
 \end{aligned}$$

where  $c$ 's are the mixing coefficients.

The partial decay width corresponding to the outgoing proton can be obtained from the overlap of the initial (parent) and the final state wave functions, which is a tensorial product of the outgoing proton and daughter wave functions, at the asymptotic limit [13]. The resulting expression is given by

$$\begin{aligned}
 \Gamma_{l_p j_p}^{I_d} &= \frac{\hbar^2 k}{\mu} \left( \frac{2I_d+1}{2I+1} \right) \left| \sum_{j_n \Omega_n \Omega_p K_d \Omega K} c_{j_n \Omega_n K_d}^{I_d} a_{\Omega_p \Omega_n \Omega K}^I \right. \\
 & \times ((I_d K_d j_p \Omega_p | I K) + (-1)^{I_d-K_d} \\
 & \times (I_d - K_d j_p \Omega_p | I K)) u_{\Omega_p} N_{l_p j_p}^{\Omega_p} \left. \right|^2, \quad (8)
 \end{aligned}$$

where  $N_{l_p j_p}^{\Omega_p} = \frac{\Phi_{l_p j_p}^{\Omega_p}(R)}{G_{l_p}(kR) + iF_{l_p}(kR)}$  is the asymptotic normalization constant comprising  $F$  and  $G$  as the regular and irregular parts of the Coulomb wave function.  $\Phi_{l_p j_p}^{\Omega_p}(R)$  is the radial part of the proton wave function having momentum vector  $k$  determined from the  $Q_p$  value.  $u_{\Omega_p}^2$  is the probability of the corresponding proton level to be empty in the daughter nucleus. The quantities in the angular brackets represent the Clebsch-Gordan coefficients. The total decay width can be obtained by summing over all the possible states as follows:

$$\Gamma^{I_d} = \sum_{j_p=|I-I_d|}^{I+I_d} \Gamma_{l_p j_p}^{I_d}, \quad (9)$$

and the corresponding half-life is obtained by  $T_{1/2} = \hbar \ln 2 / \Gamma^{I_d}$ .

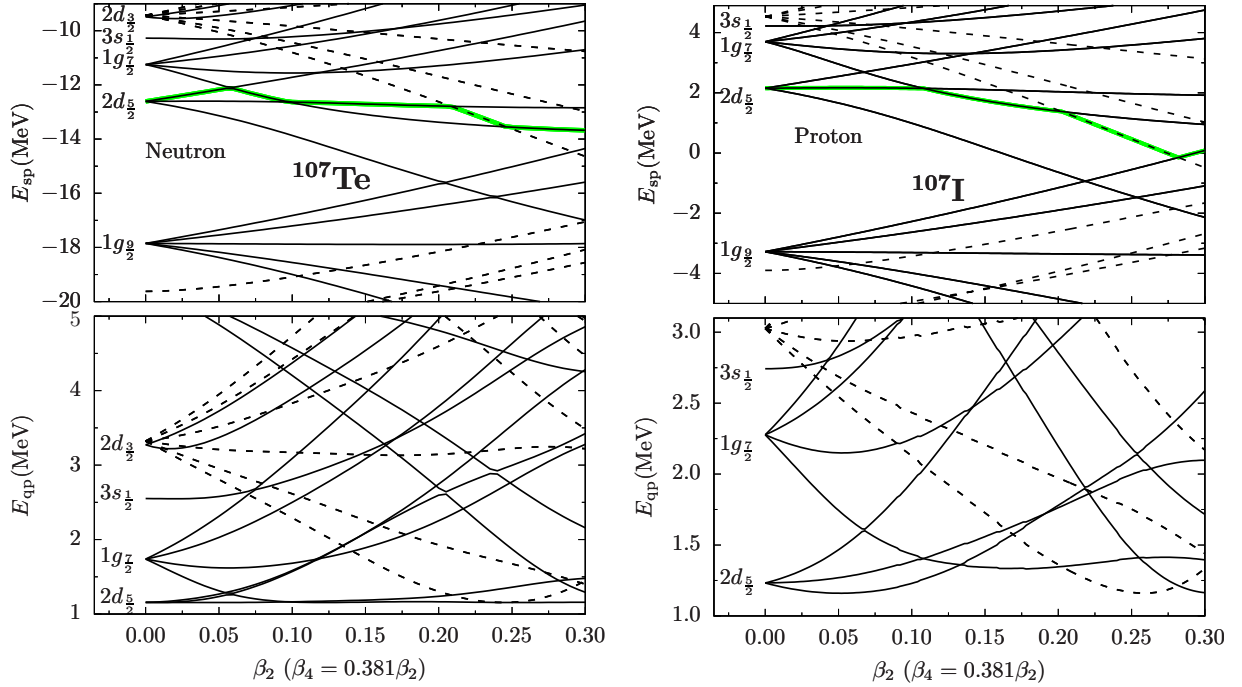


FIG. 2. Single-particle (top panels) and quasiparticle (bottom panels) levels for neutrons in  $^{107}\text{Te}$  (left) and protons in  $^{107}\text{I}$  (right) as a function of  $\beta_2$ . The solid and dashed lines correspond to the positive and negative parity states, respectively. The green lines represent the state of the valence particles. At zero deformation, the positive parity degenerate states are labeled by the quantum numbers  $nl_j$ .

**Results and discussion.** To investigate the properties of  $^{108}\text{I}$ , we utilize the formalism given in the theory section. First, we will study  $^{107}\text{Te}$ , which is the daughter of the proton emitting nucleus  $^{108}\text{I}$ . The single-particle and quasiparticle energies for neutrons in  $^{107}\text{Te}$  calculated with the parameters [14] for the Woods-Saxon potential, tuned for nuclei in this region, are given in Fig. 2. Among the positive parity levels, the orbitals of  $2d_{5/2}$  and  $1g_{7/2}$  parentage are close to the Fermi surface for a broad range of  $\beta_2$ . The identification of important levels can be done through the lowest lying quasiparticle orbitals. One can observe from the quasiparticle energies shown in Fig. 2, at  $\beta_2 \approx 0.25$ , that the orbitals of  $1g_{9/2}$  also come down. The negative parity levels of  $1h_{11/2}$  parentage are closer to the

Fermi surface only for large  $\beta_2$ . For calculating the rotational energies of  $^{107}\text{Te}$  given in Fig. 3, we have considered positive parity levels of the neutrons from the 11th up to 20th counted from the bottom, which include the single-particle levels of  $2d_{5/2}$ ,  $1g_{7/2}$ ,  $3s_{1/2}$ , and  $1g_{9/2}$  subshells. The experimental study of Ref. [15] suggests the ground state as  $5/2^+$  and the two excited states as  $7/2^+$  (90.3 keV) and  $9/2^+$  (721 keV). With  $\gamma \approx 30^\circ$ , our calculations support these assignments, since both the ordering and spacing could be reproduced, as shown in Fig. 3.

Proceeding to study the properties of  $^{108}\text{I}$ , the single-particle and quasiparticle energy levels for protons in  $^{107}\text{I}$  are shown in Fig. 2, where we observe a behavior similar

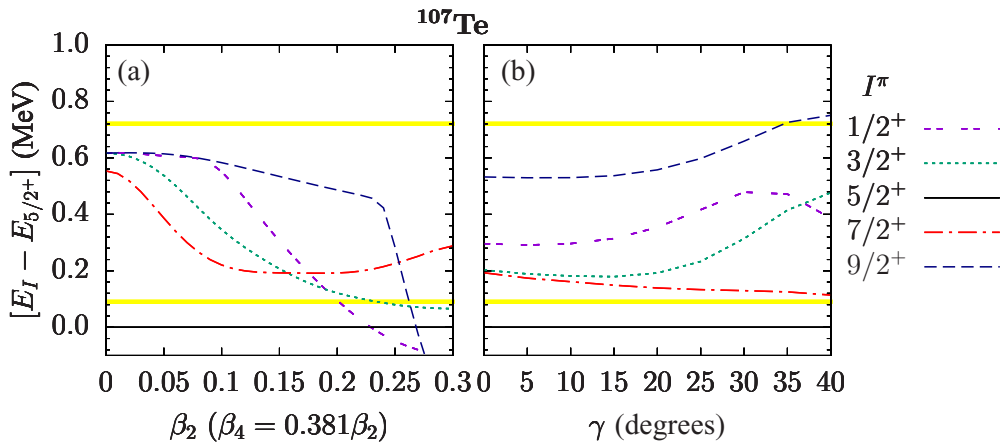


FIG. 3. Rotational energies of  $^{107}\text{Te}$  (a) with varying  $\beta_2$  and (b) with varying  $\gamma$  at  $\beta_2 = 0.152$  and  $\beta_4 = 0.058$ . Yellow lines represent the experimental data for  $7/2^+$  (lower) and  $9/2^+$  (upper) states [15].

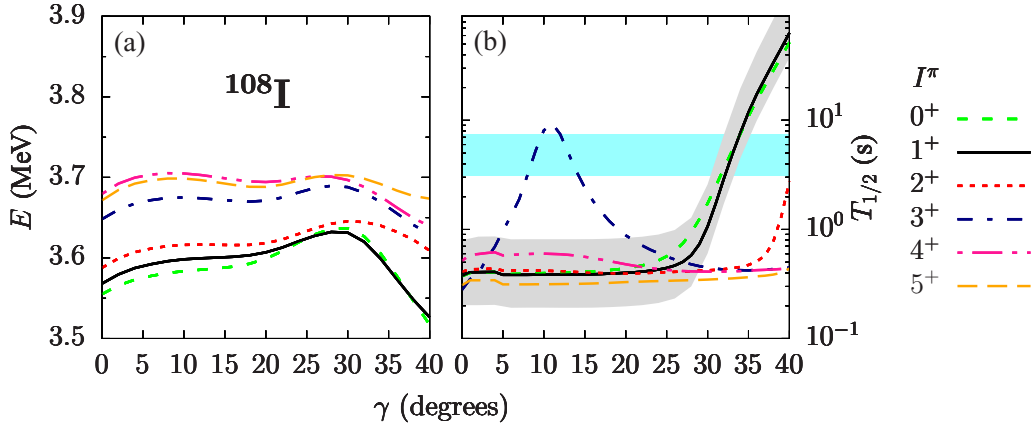


FIG. 4. (a) Rotational energies and (b) the proton emission half-life of  $^{108}\text{I}$  as a function of  $\gamma$  at  $\beta_2 = 0.152$  and  $\beta_4 = 0.058$ . The uncertainty in the calculated half-life due to the uncertainties in measured  $Q_p$  value is shown in grey. The cyan region corresponds to the experimental half-life of proton emission [1], including the error in measured data.

to the neutron levels in  $^{107}\text{Te}$ . The positive parity levels of protons from 11th to 19th (including  $2d_{5/2}$ ,  $1g_{7/2}$ ,  $3s_{1/2}$ , and  $1g_{9/2}$ ) and same neutron levels as in the case of  $^{107}\text{Te}$  are considered in our calculations. Considering axial deformation, the calculated half-lives are far from the measured ones for a broad range of  $\beta_2$ , irrespective of the residual  $np$  interaction as discussed below. Therefore, we expect that triaxiality can play a major role in  $^{108}\text{I}$ , similar to the case of  $^{109}\text{I}$  [3], and the value of  $\gamma$  will be defined as the one for which the ground state reproduces the experimental half-life. The values of  $\beta_2$  and  $\beta_4$  are considered as 0.152 and 0.058, respectively, as suggested in macroscopic-microscopic calculations [16]. However, the results do not change substantially for a broad range of  $\beta_2$ . Looking at the rotational energies of  $^{108}\text{I}$  shown in Fig. 4, one can infer that the ground state might be attributed to one of the  $0^+$ ,  $1^+$ , or  $2^+$  states for a deformation  $\gamma$  below  $30^\circ$ , while, for  $\gamma$  above  $30^\circ$ , only  $0^+$  or  $1^+$  can be a candidate.

The half-life corresponding to the proton emission from the  $3^+$  state agrees with the experimental data when  $\gamma \approx 10^\circ$ , but the energy of this state is very high from the ground state. The half-lives corresponding to  $0^+$  and  $1^+$  states are in agreement with the experimental data when  $\gamma \approx 30^\circ$ . Therefore, the inclusion of triaxiality has a substantial impact on the half-life and enables us to predict the  $\gamma$  deformation. However, the ground state spin and parity cannot be unambiguously assigned from these results. To ascertain those, we proceed to study the role of residual interaction between the valence proton and neutron.

*Role of residual neutron-proton interaction.* The residual  $np$  interaction is included in the constant potential form of Eq. (5) such that the effects of GM splitting and Newby shift are incorporated through appropriate mixing of spins, and phase factors [10].

Since the strength of residual  $np$  interaction cannot be estimated, standard values for the strength parameters are chosen to understand the corresponding qualitative effect on the ground state. As shown in Fig. 5,  $1^+$  is the lowest lying state for all sets of strength parameters, and splitting is more

enhanced between  $0^+$  and  $1^+$  at  $\gamma \approx 30^\circ$ . Also, including the GM splitting with  $V_{GM} = 0.5$  MeV, the only candidates for a ground state which are in agreement with the experimental data are the  $0^+$  and  $1^+$ , after elimination of the  $3^+$ . The  $0^+$  is predominantly singlet, and is excluded as a ground state by GM splitting and also by the Newby shift since the spin is even. Based on the above arguments related to the rotational energies and corresponding half-lives, the ground state of  $^{108}\text{I}$  can be assigned as a  $1^+$  spin and parity state, with  $\gamma \approx 30^\circ$ . Our calculations performed with a zero-range interaction [10] also supported the same conclusions.

To exclude the influence of fine structure on the decay properties, we have calculated the branching ratio for decay to the  $7/2^+$  of  $^{107}\text{Te}$ , the probable first excited state. In the considered deformation region, it was found to be very small, supporting our conclusions.

For further insight into the behavior of the rotational energies and half-lives due to the triaxial deformation and the residual  $np$  interaction, the single-particle configurations are given in Fig. 6. These configurations suggest that there is a strong mixing of many orbitals with  $1g_{7/2}$  and  $2d_{5/2}$  parentage. The sudden variation observed in the  $1^+$  state half-life at  $\gamma \approx 30^\circ$  is due to a larger contribution of the proton  $g_{7/2}$  level. When  $\gamma$  is small, the occupied level by the escaping proton is predominantly the  $d_{5/2}$ , but with increasing  $\gamma$  it is the  $g_{7/2}$  that dominates. Thus the half-life increases due to the larger centrifugal barrier.

The residual  $np$  interaction significantly affects the contribution of configurations at large  $\gamma$  for the  $0^+$  state. These effects lead to increase in the energy and half-life for this state. In the case of the  $3^+$  state, at  $\gamma = 10^\circ$  the  $np$  interaction increases the contribution of the  $\pi d_{5/2}^{[2nd]}$  level which has a larger probability  $u_{\Omega_p}^2$ , and hence reduces the half-life. The effects of residual  $np$  interaction on other states are not noticeable.

*Conclusions.* We have presented the first microscopic approach to interpret the data of triaxial odd-odd proton emitters. This nonadiabatic quasiparticle approach has been successfully applied to study the recently observed proton emission

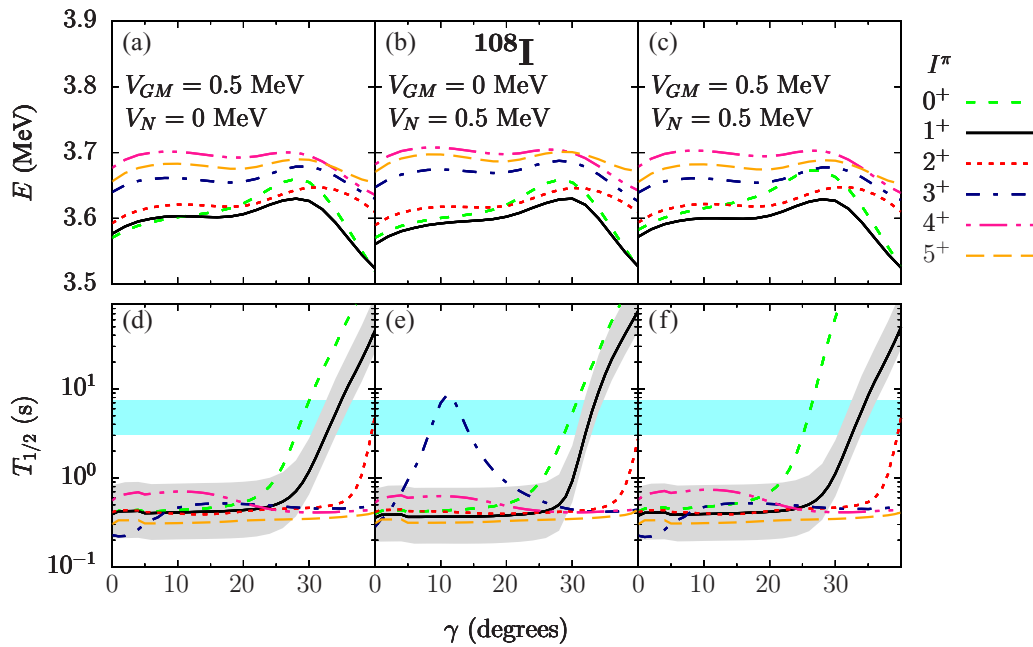


FIG. 5. Rotational energies [upper panels (a)–(c)] and the proton emission half-life [lower panels (d)–(f)] at  $\beta_2 = 0.152$ ,  $\beta_4 = 0.058$ , and as a function of  $\gamma$  calculated with different parameters (each column for a particular set of parameters) of the residual neutron-proton interaction in central potential form [Eq. (5)]. The cyan color lines correspond to the experimental proton emission half-life [1].

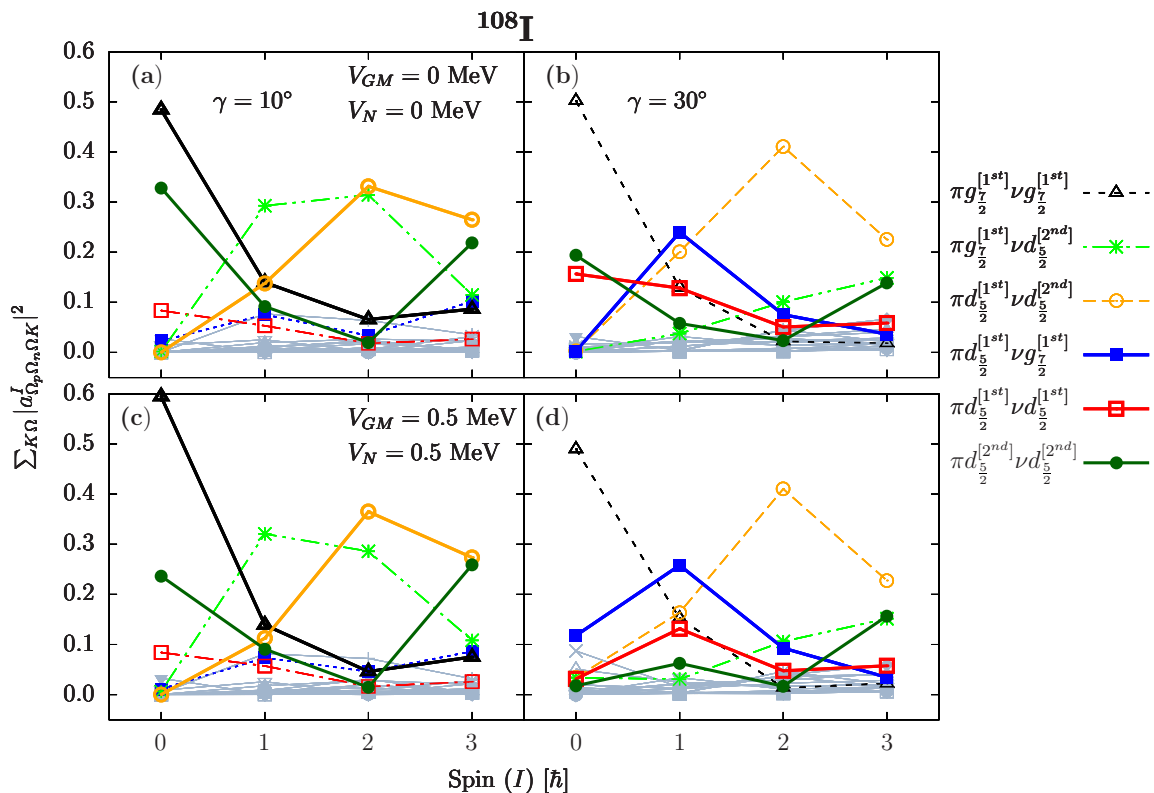


FIG. 6. The contribution of the single-particle configurations without  $np$  interaction at (a)  $\gamma = 10^\circ$ , (b)  $\gamma = 30^\circ$ , and with  $np$  interaction at (c)  $\gamma = 10^\circ$ , (d)  $\gamma = 30^\circ$  for different angular momenta ( $I$ ). The configurations which change (do not change significantly) with inclusion of  $np$  interaction at a particular  $\gamma$  are shown by solid (dashed) lines. The configurations having negligible contributions shown in grey are not labeled.

from  $^{108}\text{I}$  for the first time. The ground state spin and parity of the daughter nucleus  $^{107}\text{Te}$  is confirmed to be  $5/2^+$ . Based on the agreement of triaxiality, and the deformation is found to be  $\gamma \approx 30^\circ$ . The residual neutron-proton interaction is found to be important in assigning the spin and parity for the ground state of  $^{108}\text{I}$  by resolving the ambiguities due to the other possible states. Considering GM splitting and Newby shift, the present study suggests the  $1^+$  as the ground state from which the proton emission occurs. The analysis of single-particle

configurations revealed a strong mixing of orbitals having a  $g_{7/2}$  and a  $d_{5/2}$  origin, rather than dominance by a particular orbital angular momentum. This result settles the relevant uncertainties pointed out in Ref. [1]. The mixed configurations in  $^{108}\text{I}$  might also be present in the neighboring nuclei involved in the end cycle of the  $rp$  process, and have to be treated in a nonadiabatic manner.

*Acknowledgments.* The authors P.A. and S.M. acknowledge support from the TEQIP Collaborative research scheme, MHRD, Govt. of India, via Project No. ID 1-5728195591.

- 
- [1] K. Auranen, D. Seweryniak, M. Albers, A. Ayangeakaa, S. Bottoni, M. Carpenter, C. Chiara, P. Copp, H. David, D. Doherty, *et al.*, *Phys. Lett. B* **792**, 187 (2019).
- [2] V.-V. Elomaa, G. K. Vorobjev, A. Kankainen, L. Batist, S. Eliseev, T. Eronen, J. Hakala, A. Jokinen, I. D. Moore, Y. N. Novikov, *et al.*, *Phys. Rev. Lett.* **102**, 252501 (2009).
- [3] S. Modi, M. Patial, P. Arumugam, E. Maglione, and L. S. Ferreira, *Phys. Rev. C* **95**, 054323 (2017).
- [4] C. Mazzocchi, R. Grzywacz, S. N. Liddick, K. P. Rykaczewski, H. Schatz, J. C. Batchelder, C. R. Bingham, C. J. Gross, J. H. Hamilton, J. K. Hwang, *et al.*, *Phys. Rev. Lett.* **98**, 212501 (2007).
- [5] B. Blank and M. J. G. Borge, *Prog. Part. Nucl. Phys.* **60**, 403 (2008).
- [6] G. Fiorin, E. Maglione, and L. S. Ferreira, *Phys. Rev. C* **67**, 054302 (2003).
- [7] P. Arumugam, L. S. Ferreira, and E. Maglione, *Phys. Lett. B* **680**, 443 (2009).
- [8] M. Patial, P. Arumugam, A. K. Jain, E. Maglione, and L. S. Ferreira, *Phys. Lett. B* **718**, 979 (2013).
- [9] S. Modi, M. Patial, P. Arumugam, E. Maglione, and L. S. Ferreira, *Phys. Rev. C* **95**, 024326 (2017).
- [10] P. Siwach, P. Arumugam, S. Modi, L. S. Ferreira, and E. Maglione, *J. Phys. G: Nucl. Part. Phys.* **47**, 125105 (2020).
- [11] C. J. Gallagher, Jr. and S. A. Moszkowski, *Phys. Rev.* **111**, 1282 (1958).
- [12] N. D. Newby, *Phys. Rev.* **125**, 2063 (1962).
- [13] L. S. Ferreira and E. Maglione, *Phys. Rev. Lett.* **86**, 1721 (2001).
- [14] H. Esbensen and C. N. Davids, *Phys. Rev. C* **63**, 014315 (2000).
- [15] B. Hadinia, B. Cederwall, K. Lagergren, J. Blomqvist, T. Bäck, S. Eeckhaudt, T. Grahn, P. Greenlees, A. Johnson, D. T. Joss *et al.*, *Phys. Rev. C* **70**, 064314 (2004).
- [16] P. Moller, R. Bengtsson, B. Carlsson, P. Olivius, T. Ichikawa, H. Sagawa, and A. Iwamoto, *At. Data Nucl. Data Tables* **94**, 758 (2008).